16TH EUROPEAN CONFERENCE ON EARTHQUAKE ENGINEERING THESSALONIKI 18 - 21 JUNE 2018

NUMERICAL AND EXPERIMENTAL INVESTIGATION ON LOW DAMAGE STEEL-TIMBER POST-TENSIONED BEAM-COLUMN CONNECTION

Murilo José Mancini[1], Stefano Pampanin[2]

ABSTRACT

The use of engineered timber for Moment Resisting Frames (MRF) has undergone a significant evolution in the past years. In particular, the use of post-tensioned cables has allowed the development of moment-resisting jointed ductile connections for multi-story concrete, steel or timber frames in seismic areas. Post-tensioned cables/bars passing through the beam-column connections allow the self-centering of the frames after a seismic event. Also, the use of dissipative devices adds damping and ductility at the connection, developing a peculiar “flag-shape” hysteretic behavior. From the combination of these two features arises a connection referred to as "Hybrid System" using the term adopted in the 1990s as part of the PRESSS (PREcast Seismic Structural Systems) program. This technology concentrates inelastic demand at the connection level (gap opening) allowing damage control.

A significant enhancement in the potentiality of this technology has been the extension to engineered wood material (Glulam/LVL), referred to as Pres-Lam (Prestressed-Laminated) timber. In this case, attention has to be given in orthotropic behavior (connection interface) and solutions to provide higher axial strength to the vertical elements are required (tall buildings development).

In this paper, the results of a numerical and experimental campaign are presented for the development and validation of a hybrid material configuration of a Post-Tensioned beam-column connection: steel column and timber beam. The numerical FEM model was first validated on past experimental tests on Timber-Timber connection configurations using Glulam and LVL. Quasi-static cyclic tests were carried out on an 80% scale Steel column and Timber beam post-tensioned connection.

Keywords: Post-tensioned timber; Rocking conections; PRESSS; Pres-Lam; Damage-control

1. INTRODUCTION

In addition to base isolation and supplemental damping solutions, low damage technologies in earthquake engineering have been enhanced with the introduction of the “Hybrid connection” that combines two features: Self-centering and Hysteretic dissipation (Priestley et al., 1999) generating a “flag-shape” hysteretic rule. Unbonded post-tensioned bars/tendons provide the self-centering capability and partially unbonded mild-steel internal bars or externally replaceable dissipaters provide the energy dissipation characteristics. In a lateral loading (seismic event) a controlled rocking mechanism is activated maintaining all the structural parts under elastic domain except the mild-steel (or alternative solution) “dissipaters”, that undergoing inelastic domain, offer dissipation to the system (Figure 1).
Further enhancement was achieved with the extension of this technology to timber structures in the early 2000s, at University of Canterbury, extensive experimental and analytical/numerical campaigns were performed on frame and wall systems in order to develop and validate a new solution for multi-storey timber (engineered wood) buildings, referred to as Pres-Lam (Palermo et al., 2005).
Further large scale experimental tests using LVL (Iqbal et al., 2010);(Newcombe et al., 2010), Glulam

[1]PhD Candidate, University of Rome ‘La Sapienza’, Italy, murilo.mancini@uniroma1.it
[2]Full Professor, University of Rome ‘La Sapienza’, Italy, stefano.pampanin@uniroma1.it

(Smith et al., 2013) and CLT (Dunbar et al., 2014) were performed in order to validate this technology to various engineered wood materials.

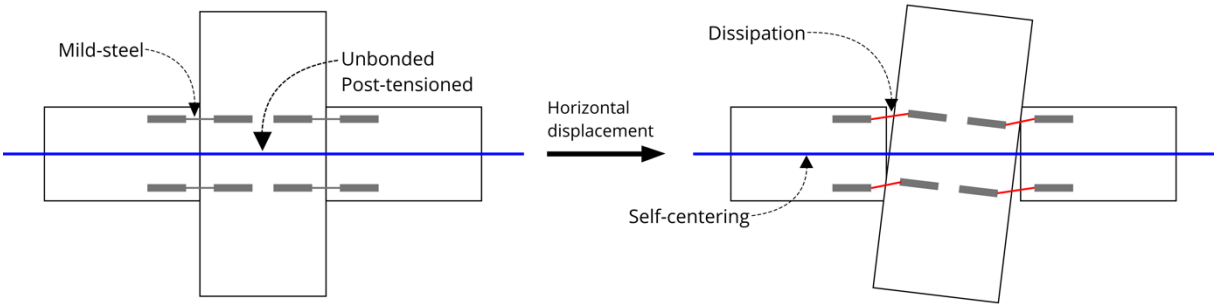

Figure 1 - Hybrid connection behavior.

The main objective of the research herein presented is to provide an alternative and efficient solution to some inherent drawbacks of a timber-timber frame system, namely the effects of perpendicular-to-grain loading to the column and the limited E-modulus and axial strength of timber columns for high-rise buildings (i.e. higher than 10-15 storeys). Emulating the CFT (concrete-filled-tube) column solutions highly adopted at international level for high-rise buildings, in this research, the feasibility of a steel-column and timber beam configurations have been investigated.

The methodology adopted in this research comprises the following steps: (a) validation of a Finite Element (FE) numerical model for full timber connections (b) presentation of a new hybrid material configuration for unbonded Post-tensioned connections: Steel column with Timber beam using FE numerical models; (c) Experimental quasi-static cyclic tests on a large scale Steel column and Timber beam post-tensioned connection.

2.MOMENT CAPACITY PROCEDURES

The moment-rotation capacity of post-tensioned jointed ductile concrete connection can be obtained by procedures available in literature (Pampanin et al., 2001 and Palermo & Pampanin, 2008). On the other hand, for moment-rotation capacity using timber structures, few procedures were adopted in order to reproduce its features, as flexibility, ductility and others. Specific guidelines for the design and modeling analysis of unbonded post-tensioned timber (Pres-Lam) structures have been prepared by Pampanin (2013) (Pampanin et al., 2013).

In order to obtain gap opening prediction, the elastic rotations of structural parts and the joint interface rotation have to be discounted from the design drift.

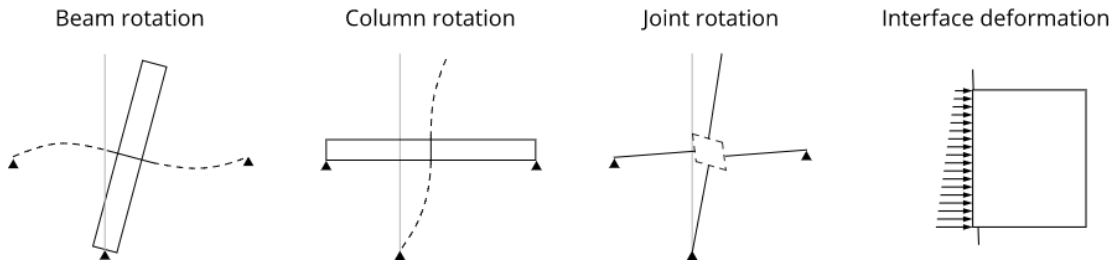

Figure 2 – Rotation contributions to a total Post-tensioned timber connection rotation (modified from Van Beerschoten, 2011).

The estimation of the gap opening is obtained using specified equations presented below. This analytical method is described in more details the “Post-Tensioned Timber Buildings Design Guide” for Australia and New Zealand (Pampanin et al., 2013).

$$\theta_{con} = \theta_d - \theta_b - \theta_c - \theta_j \quad (1)$$

with θ_d *= drift design;* θ_b *= beam rotation;* θ_c*, column rotation;* θ_j*, joint rotation.*

The elastic rotations can be calculated with deflection equations from simple beam theory, using the moment demand from the building design. The gap opening (θ_{imp}) can be obtained with equations below:

$$\theta_{imp} = \theta_{con} - \theta_{int} \quad (2)$$

$$\theta_{int} = 0{,}2\,\frac{2T_{pt,initial}.h_c}{E_{perp}h_b^2 b_b} \quad (3)$$

Being: θ_{imp}*, gap opening (imposed rotation);* θ_{int}*, interface rotation;* $T_{pt,initial}$*, Initial applied post-tensioned force;* h_c*, Column depth;* E_{perp}*, Young modulus perpendicular to the grain;* h_b*, Beam depth;* b_b*, Beam width.*

It is noted that as the gap opens, the post-tensioned bar elongates and increase the post-tensioning force. With this, the rotation interface (θ_{int}) increases and it is thus not a constant. It is recommended to use, iteratively, the equation below:

$$\theta_{int} = 0{,}2\,\frac{2T_{pt}.h_c}{E_{perp}h_b^2 b_b} \quad (4)$$

Timber-to-timber beam-column connections are more susceptible to decompression effects at the interface connection before the opening of the gap (Van Beerschoten, 2011). The Monolithic Beam Analogy (MBA) originally developed by Pampanin (Pampanin et al., 2001) and further refined into a Modified MBA, or MMBA, by Palermo (Palermo et al., 2004) can be used to calculate the moment-rotation behavior of a rocking connection. This method, initially developed for precast concrete connection, introduces an analogy to a monolithic beam to obtain a member compatibility condition and derive deformation and stresses at the connection interface. An extension of the method for timber rocking connections has been presented in Newcombe et al., 2008. The general method consists of: estimation of the neutral axis position c, evaluation of strain, stresses and forces in mild-steel, post-tensioned bars and timber fibers, equilibrium evaluation and iteration on the neutral axis position.

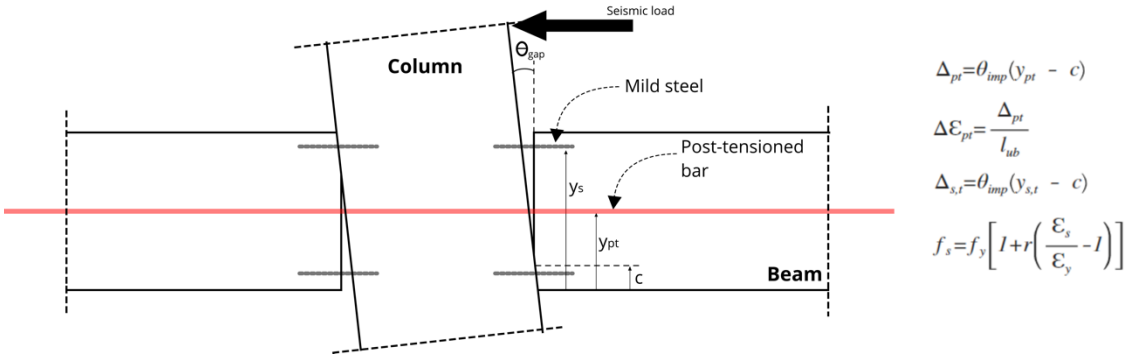

Figure 3 – Gap Opening mechanisms and notations according to a MBA and MMBA procedure.

3.NUMERICAL MODEL EVALUATION

A Finite Element Model using 3D elements (8 node linear solid, reduced integration, hourglass control and 6 node solid, linear triangular prism) was implemented within ABAQUS (SIMULIA, ABAQUS 6.14) to simulate hybrid post-tensioned beam-column connections. To validate the model the experimental tests realized with Glulam and LVL (Smith et al., 2013, Newcombe et al., 2008) were replicated.

a) b) 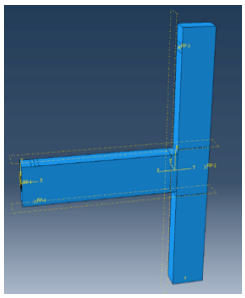 c) 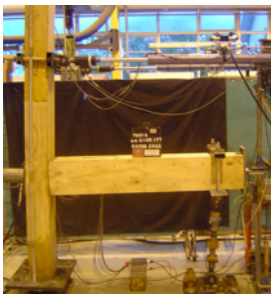 d) 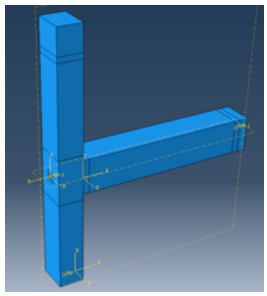

Figure 4 - a) Experimental tests realized with Glulam (Smith et al., 2013); b) Numerical model based on (a); c) Experimental tests realized with LVL (Newcombe et al., 2008); d) Numerical model based on (c).

The orthotropic behavior of timber was considered and the mechanical characteristics of the steel and timber materials were assumed as indicated in the tables below.

Table 1 - Mechanical characteristics of HySpan – LVL.

		HySpan	
Modulus of Elasticity parallel to the grain	E_{par}	13200	MPa
Modulus of Elasticity perpendicular to the grain	E_{perp}	660	MPa
Modulus of Rigidity	G	660	MPa
Bending Strength	f'_b	48	MPa
Tension parallel to the grain	f'_t	33	MPa
Compression parallel to the grain	f'_c	45	MPa
Shear in beams	f'_s	5.3	MPa
Compression perpendicular to the grain	f'_p	12	MPa
Shear at joint details	f'_{sj}	5.3	MPa

Table 2 - Post-tensioned strands mechanical properties (LVL experiment).

Nominal diameter	D_{nom}	*13*	*mm*
Nominal Area	A_{pt}	99	mm^2
Ultimate stress	f_{pu}	1862	MPa
Elastic Modulus	E_{pt}	197	GPa
Yield stress	f_{py}	1560	MPa

Table 3 - Mechanical properties of Glulam - GL32h

		GL32h	
Modulus of Elasticity parallel to the grain	E_{par}	11100	MPa
Modulus of Elasticity perpendicular to the grain	E_{perp}	460	MPa
Modulus of Rigidity	G	850	MPa
Bending Strength	f'_b	32	MPa
Compression parallel to the grain	f'_c	29	MPa
Shear in beams	f'_s	3.8	MPa
Compression perpendicular to the grain	f'_p	3.3	MPa

Table 4 - Mechanical characteristics of post-tensioned tendons (Glulam experiment)

Nominal diameter	D_{nom}	*15.2*	*mm*
Nominal Area	A_{pt}	181	mm^2
Ultimate stress	f_{pu}	1760	MPa
Elastic Modulus	E_{pt}	201	GPa
Yield stress	f_{py}	1530	MPa

At the beam-column interaction a linear interface softening simulation was considered in order to represent the end-effect behavior of timber. A pressure-overclosure coefficient was calibrated based on

neutral-axis position defined on analytical formulation. The neutral-axis final position (2.5% drift) from numerical model was plotted in function of pressure-overclosure coefficient in order to define, through correlation curves, correspondent pressure-overclosure coefficient used on numerical model. Pressure overclosure coefficient charts can be visualized in Figure 5.

With the equation $k = A.\left(\frac{c}{h}\right)^B$ (5), based on correlation curves on Figure 5, it is possible to obtain an accurate pressure-overclosure coefficient (k) to be used for the softening interface of the numerical model. With these variables available it was possible to validate the numerical model against past experimental campaigns and analytical equations.

$$k = A.\left(\frac{c}{h}\right)^B \quad (5)$$

Being: A and B coefficients from correlation curves.

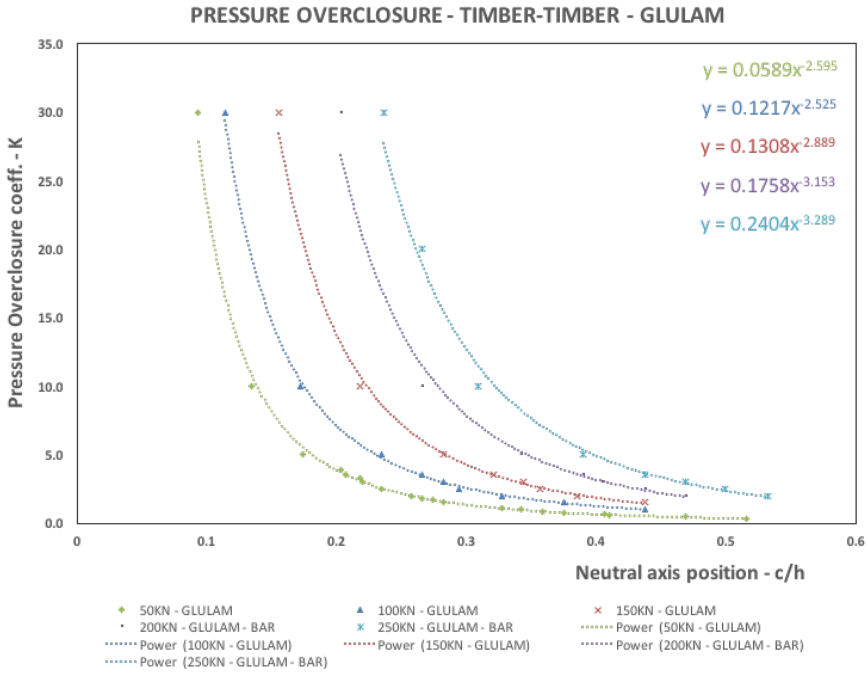

Figure 5 - Pressure overclosure calibration method for numerical model

Figures 6-9 show an experimental vs analytical and numerical models for various test campaigns.

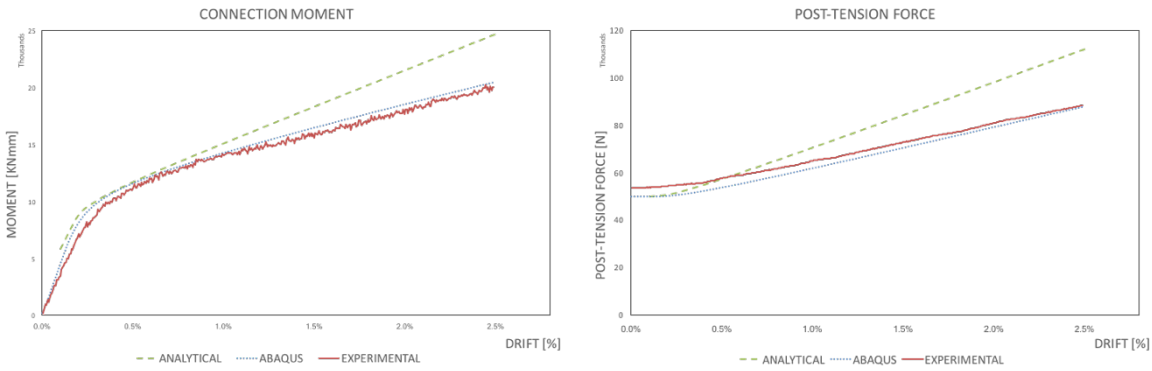

Figure 6 – Analytical, numerical and experimental comparison - 50kN post tension only with Glulam

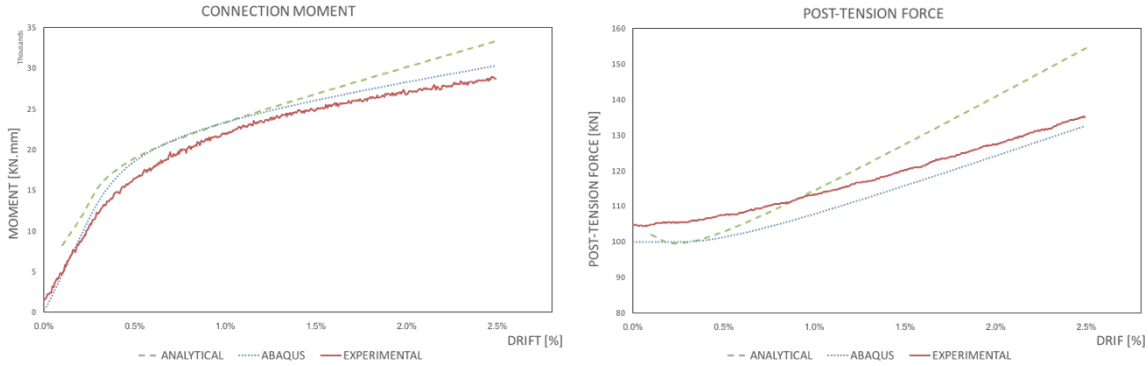

Figure 7 - Analytical, numerical and experimental comparison -100kN post tension only with Glulam

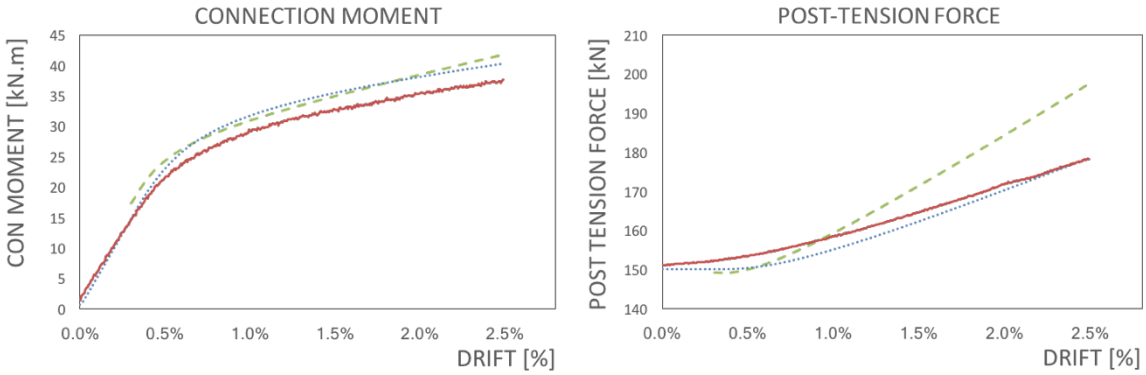

Figure 8 - Analytical, numerical and experimental comparison -150kN only post tensioned with Glulam

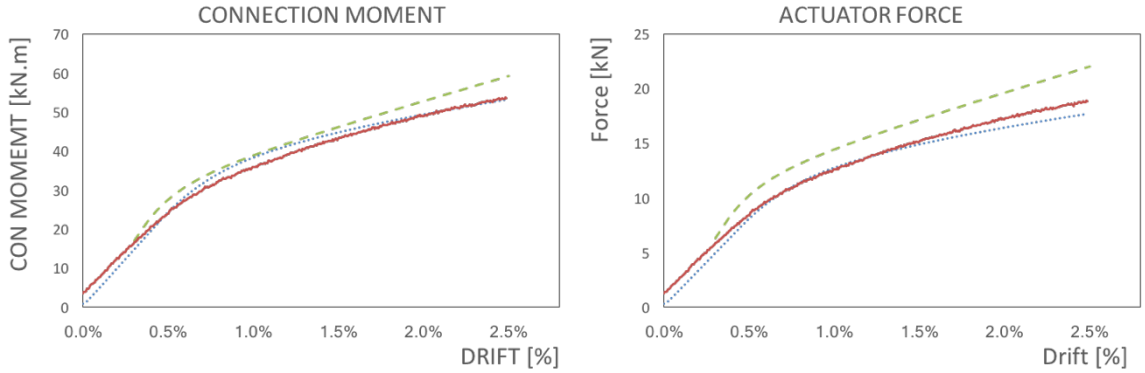

Figure 9 - Analytical, numerical and experimental comparison -200kN only post tensioned with Glulam

The numerical model provided satisfactory results in terms of post-diction of the behavior of timber-timber configuration, arguably the more complicated to capture due to the perpendicular to grain effects, albeit often reduced in the testing campaigns by some type of armoring or reinforcing of the joint region through screws, plates etc. In the next phases the model was thus extended to predict the behavior of the new steel column to timber beam configurations

In parallel with the numerical modeling an experimental campaign on beam-column exterior joints was prepared with the objective to evaluate and verify this enhancement. A building prototype, described in the following section, was used to derive the geometric properties of the specimens.

4. BUILDING PROTOTYPE

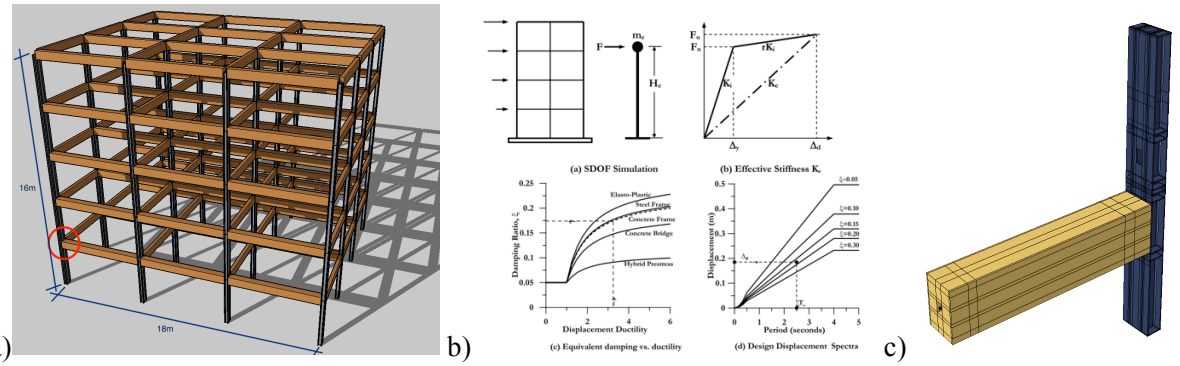

a) b) c)

Figure 10 - a) Building prototype; b) Direct Displacement Based Design procedures (Priestley et al., 2007); c) Steel-timber beam-column connection numerical model.

The building prototype consist of a 5 storeys frame structure with three 6m bays in the longitudinal direction (18m total), 3.2 m inter-story height (16m total). A seismic weight of 10kN/m^2 on floors with an approximated area of 270m^2/floor was considered. The seismic hazard and design spectra were assumed according to the *NZS 1170.5* (2004) with a Z=0.3 and soil type D. Steel columns and Glulam post-tensioned timber beams are adopted. The post-tensioning system consist of high strength bars (DYWIDAG/SAS).

A Direct Displacement Based Design (DDBD) (Priestley et al., 2007) with a 2.5% design drift was adopted to define the internal action, i.e. moment demand, in the steel-timber building prototype frame. For design purposes unidirectional frames were considered the only lateral resisting system. The main objective here is to investigate the beam-column connection behavior.

5. EXPERIMENTAL AND NUMERICAL CAMPAIGN

For experimental purposes, the beam-column subassembly model was scaled to 80%. For this scaling the Cauchy-Froude similitude method was adopted. The experimental tests were carried out at the Structural Laboratory of the University of Rome 'La Sapienza'. The test set-up and geometrical properties are show in Figure 11.

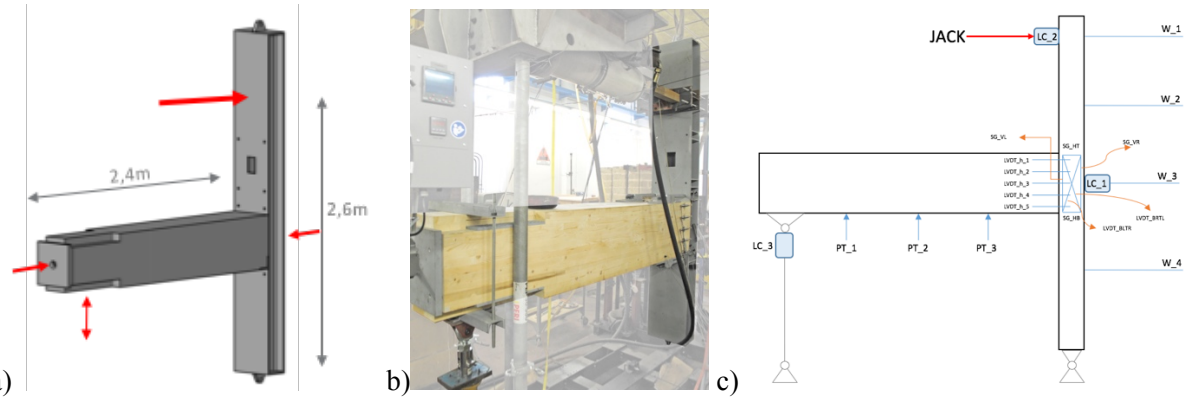

a) b) c)

Figure 11 - a) Experimental set-up; b) Specimen assembled inside laboratory; c) Instrumentation set-up.

A Schenk hydraulic actuator (250kN capacity) was used to apply a displacement controlled loading protocol at the column contra-flexure point, consisting of a modified version of the ACI load protocol [ACI T1.1-01 & ACI T1.1R-01 2001; ACI T1.2-03 2003], with two cycles at each increasing drift level until 2.5% maximum drift.

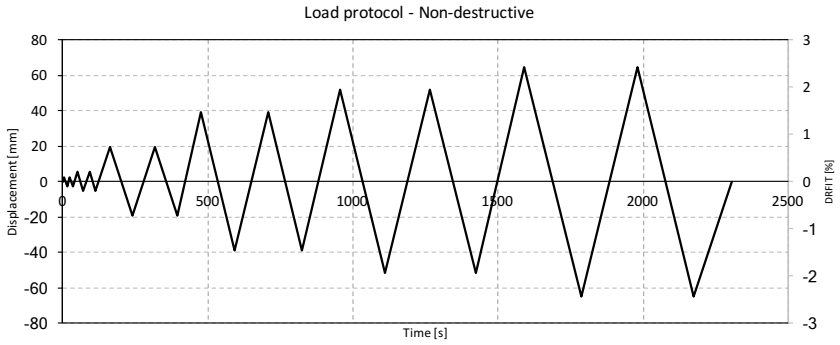

Figure 12 – Displacement/drift-control quasi-static loading protocol.

Four series of tests have been so far carried out with only post-tensioned bars varying its initial post-tensioning: 50kN, 100kN, 150kN and 200kN. The tests were realized with the objective to visualize and validate the new configuration connection that uses mixed material. The instrumentation, shown in Figure 11(c), consisted of LVDTs to measure the gap opening at the interface and the neutral axis position, potentiometers at beam and column to measure elastic rotation of these structural components, 6 strain-gauges to measure the deformation at joint panel and 3 load cells to measure the applied forces by the actuator, the post-tensioned bar and the vertical reaction in the beam at the contra-flexure point. The material properties adopted in the experimental campaign are summarized in Tables 5-7.

Table 5 - Mechanical characteristics of Glulam GL32h used in experimental campaign.

Glulam GL32h – Beam			
Modulus of Elasticity parallel to the grain	E_{par}	13700	MPa
Modulus of Elasticity perpendicular to the grain	E_{perp}	460	MPa
Modulus of Rigidity	G	850	MPa
Bending Strength	f'_b	32	MPa
Tension parallel to the grain	f'_t	22.5	MPa
Compression parallel to the grain	f'_c	29	MPa
Shear in beams	f'_s	3.8	MPa
Compression perpendicular to the grain	f'_p	3.3	MPa

Table 6 - Mechanical characteristics of Steel S355

Steel S355 - Column			
Modulus of Elasticity	E	210	GPa
Shear modulus	G_t	80	GPa
Yield strength	f_y	355	MPa
Ultimate Strength	f_u	490	MPa

Table 7 - Mechanical properties of high strength steel bar used for post-tensioned system

High strength post-tensioned bar (SAS)			
Modulus of Elasticity	E	170	GPa
Yield strength	f_y	1050	MPa

5.1 EXPERIMENTAL RESULTS

From the first series of experiments the results confirmed the expectations, highlighting the high stiffness in the column at the connection region when compared to a timber-timber equivalent configuration. The gap opening developed as predicted with practically no residual deformation and minimum post-tension losses.

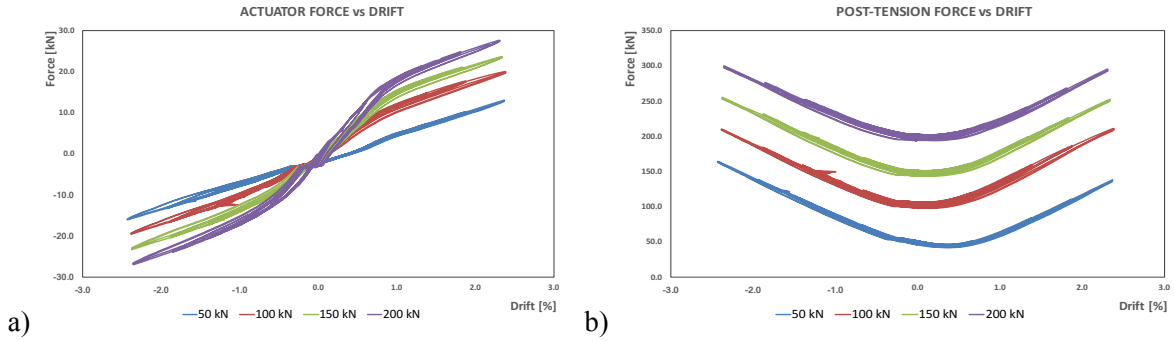

a) b)

Figure 13 - a) Actuator force vs drift; b) Force in the post-tensioned cable vs drift

In Figure 13(b) the increase in post-tension forces with the gap opening is observed. Important to highlight that the system remain fully elastic, considering that, at this point there were no additional dissipation devices. The non-linear behavior is due to geometric non-linearity typical of a rocking mechanism.

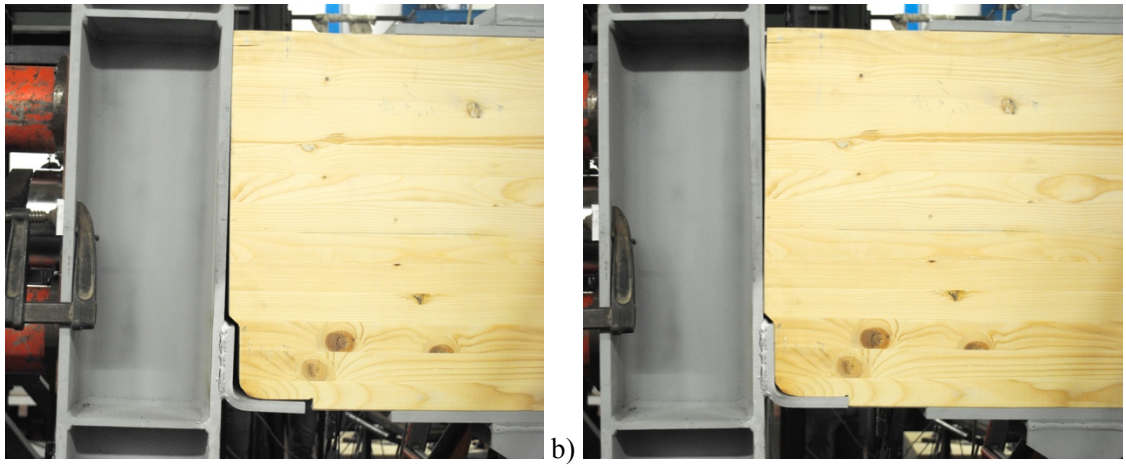

a) b)

Figure 14 - Gap opening during the experimental tests (2.5% drift).

5.2 NUMERICAL MODEL

A numerical model was created using ABAQUS as FE software solver and the model was evaluated based on past experimental tests and enhanced for new configuration using mixed material. 3D elements were created with the intent to observe stresses and strains path through the system. With this model created was possible to observe connection behavior and predict (blind) results. Posteriorly the model was compared with analytical formulation and experimental tests in order to evaluate the model for Steel-Timber configuration.

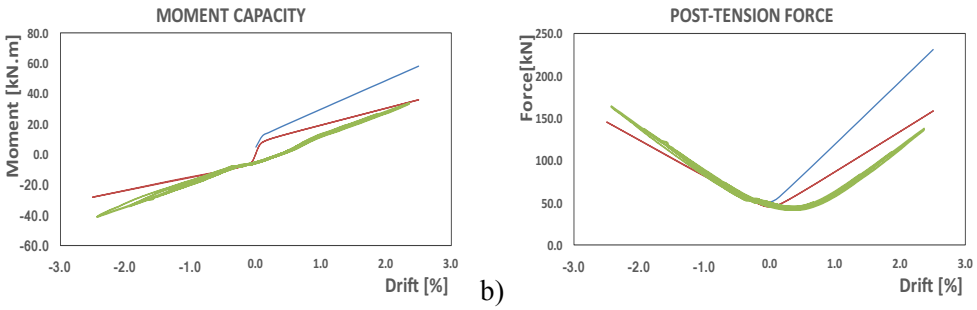

a) b)

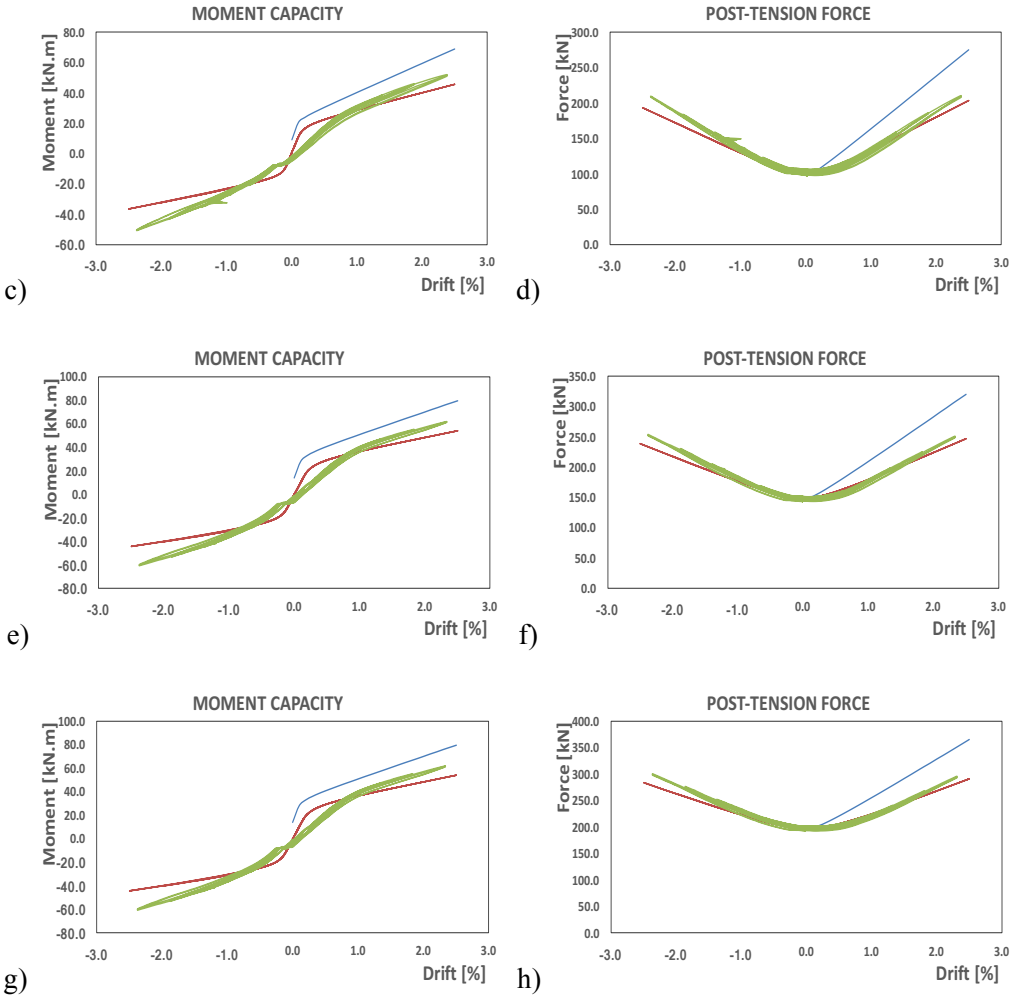

Figure 15 - Comparative results among analytical, numerical and experimental with Steel-Timber connection. (a) and (b) - 50kN only post-tension. (c) and (d) - 100kN only post-tension. (e) and (f) – 150kN only post-tension. (g) and (h) – 200kN only post-tension.

It is possible to observe in comparative results, discrepancy, in higher drifts, in analytical formulation. Analytical equations do not consider local deformations in the system. Thus, it is expected this behavior. Figure 16 shows the gap opening mechanism and strain distribution predicted by the FE numerical model. The qualitative trend behavior can be observed in Figure 14.

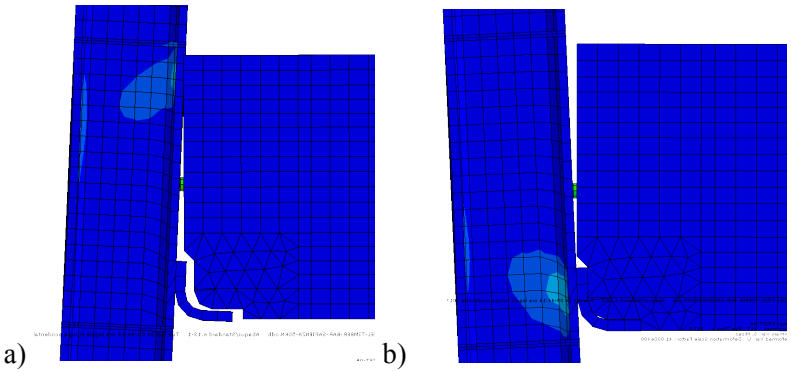

Figure 16 - FE Numerical model – gap opening mechanism and strain distribution (2.5% drift)

5.2.1 – NUMERICAL SIMULATION OF EXTERNAL FUSED DISSIPATERS

External fused-type or 'Plug&Play' dissipaters were simulated in the numerical FE model using Spring/Dashpot coefficients in order to emulate real dissipaters. To fully implement 3D elements

representing dissipaters in the numerical model would require excessive processing power and computational time. As a compromise, at this stage, "wired elements" were created to simulate those dissipaters. A simple hysteretic cycle was used to represent mechanical behavior of this element. See Figure below.

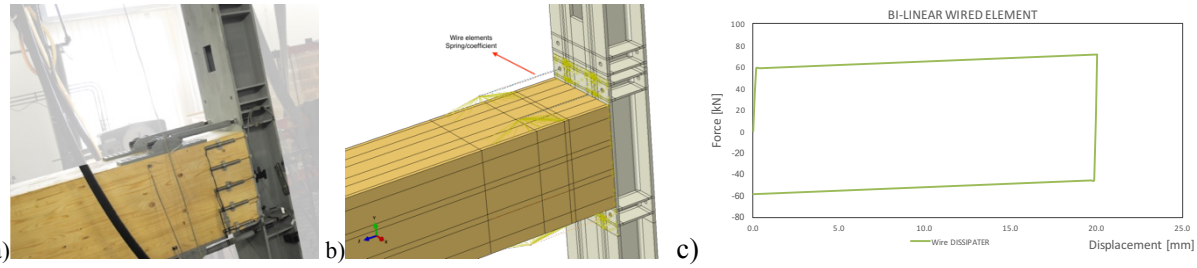

Figure 17 – Numerical model with dissipaters: (a) External fused 'Plug&Play' dissipaters assembled at part of the experimental set-up; (b) Wired elements simulating within the numerical model the external fused 'Plug&Play' dissipaters; (c) simplified hysteretic cycle of wired element dissipater.

At this stage few tests were analyzed with the main intent to represent the hybrid connection. Further models will be tested in parallel to the following experimental campaign on hybrid post-tensioned dissipative solution including external fused dissipaters at the connection. After all, it will be possible to compare and calibrate the numerical model using the previously mentioned simplified wired dissipaters solution.

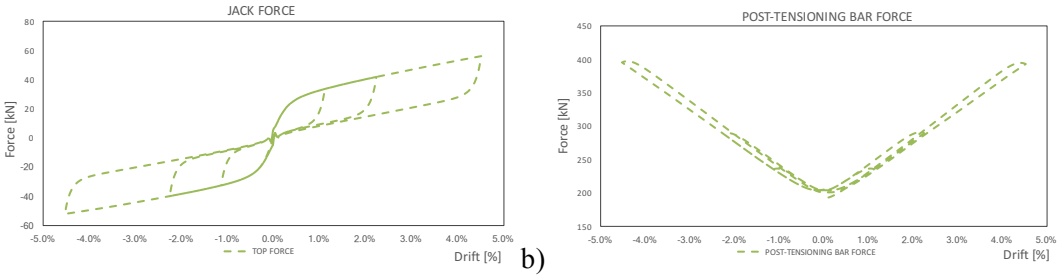

Figure 18 – Numerical prediction of the expected flag-shaped behavior of the post-tensioned dissipative connection when using the simplified 'wired' numerical element to simulate the external fused 'Plug&Play' dissipaters.

6. CONCLUSIONS

This paper presented the experimental and numerical investigations on a low-damage beam-column connection with timber-timber and/or steel-timber configurations. A FE numerical model was developed in ABAQUS with 3D solid elements in the simulation of Timber-Timber connections (model evaluation) and Steel-Timber connections (moment capacity and behavior predictions). The experimental campaign on a series of large scale beam-column specimen subject to quasi-static cyclic loading, has been carried out (and still in progress) at the Structural Laboratory of the University of Rome 'La Sapienza' in order to evaluate the feasibility and performance of the new steel-timber hybrid configuration.

Overall the new configuration of Steel-Timber post-tensioned connection showed a very satisfactory performance with minor stiffness degradations, negligible losses of post-tensioned force and residual deformation after removing the lateral force. Due to the lack of perpendicular-to-grain loading in the steel column, local deformation effects due to the so-called interface deformation are minimal.

Improvements of the corbel/shear keys configuration are required. The version adopted herein had the advantage of being constructed as a typical supporting cleat and being architecturally 'hidden', but resulted into a complicated manufacturing end-detailing in the beam element and produced a non-symmetric behavior interfering with the rocking motion. At the time of writing, the experimental tests are continuing with the addition of external replaceable fuse-type or "Plug&Play" dissipaters.

The numerical model simulations using simplified wired elements to model the dissipaters are predicting a satisfactory dissipative-recentering behavior with a stable flag-shape hysteresis rule.

7. ACKNOWLEDGMENTS

The research herein presented is part of the project “Seismic Safety and Sustainability: Innovative Technologies and Integrated Design for Multi-storey Open-space Timber Buildings” funded by Sapienza University of Rome (Progetto di Ateneo Medio 2016).
The first author’s PhD Scholarship has been provided by the Erasmus Mundus Program.
The collaboration and financial support provided by LA COST Srl in the manufacturing and delivering of the beam-column joint specimens is greatly acknowledged.

8. REFERENCES

Dunbar, A. J. M. (2014). Seismic design of core-wall systems for multi-storey timber buildings.

Iqbal, A., Pampanin, S., Palermo, A., & Buchanan, A. H. (2010). Seismic performance of full-scale post-tensioned timber beam-column joints. In *11th World Conference on Timber Engineering 2010, WCTE 2010* (Vol. 4, pp. 2948–2957).

Newcombe, M. P., Pampanin, S., & Buchanan, A. H. (2010). Experimental testing of a two-storey post tensioned timber building. In *9th US National and 10th Canadian Conference on Earthquake Engineering 2010, Including Papers from the 4th International Tsunami Symposium* (Vol. 1, pp. 273 282).

Newcombe, M. P., Pampanin, S., Buchanan, A., & Palermo, A. (2008). Section Analysis and Cyclic Behavior of Post-Tensioned Jointed Ductile Connections for Multi-Story Timber Buildings. *Journal of Earthquake Engineering*, *12*(sup1), 83–110.

NZS 1170.5 - Structural design actions - Part 5: Earthquake actions. (2004). *Standards New Zealand.*

Palermo, A., & Pampanin, S. (2008). Analysis and Simplified Design of Precast Jointed Ductile Connections. *The 14 Th World Conference on Earthquake Engineering*.

Palermo, A., Pampanin, S., & Calvi, G. M. (2004). Use of “Controlled Rocking” in the seismic design of Bridges. *13th World Conference on Earthquake Engineering*, (4006), Paper No. 4006.

Palermo, a, Pampanin, S., Buchanan, a, & Newcombe, M. (2005). Seismic design of multi-storey buildings using laminated veneer lumber (LVL). *NZSEE Conference*, (Xxx).

Pampanin, S., Palermo, A., & Buchanan, A. (2013). *Design guide Australia and New Zealand - POST TENSIONED TIMBER BUILDINGS - Part1,2,3*.

Pampanin, S., Palermo, a., & Buchanan, A. (2013). POST-TENSIONED TIMBER BUILDINGS

Pampanin, S., Priestley, M. J. N., & Sritharan, S. (2001). Analytical modelling of the seismic behaviour of precast concrete frames designed with ductile connections. *Journal of Earthquake Engineering*, *5*(3), 329–367.

Priestley, M., Calvi, G. M., & Kowalsky, M. J. (2007). Displacement-based seismic design of structures. *Building*, *23*(33), 1453–1460.

Priestley, M. J. N., Sritharan, S. S., Conley, J. R., & Pampanin, S. (1999). Preliminary results and conclusions from the PRESSS five-story precast concrete test building. *PCI Journal*, *44*(6), 42–67.

Priestley, & Kowalsky. (2000). Direct-displacement based design of concrete buildings. *Bulletin of the New Zealand Society for Earthquake Engineering*.

SIMULIA. (n.d.). ABAQUS 6.14 - Documentation.

Smith, T., Ponzo, F. C., Di Cesare, A., Pampanin, S., Carradine, D., Buchanan, A. H., & Nigro, D. (2013). Post-Tensioned Glulam Beam-Column Joints with Advanced Damping Systems: Testing and Numerical Analysis. *Journal of Earthquake Engineering*, *18*(1), 147–167.

Van Beerschoten, W. (2011). Structural performance of post-tensioned timber frames under gravity loading.